Cement mantle fatigue failure in total hip replacement: Experimental and computational testing

Published in:
Journal of Biomechanics

Document Version:
Early version, also known as pre-print

Queen's University Belfast - Research Portal:
Link to publication record in Queen's University Belfast Research Portal

Cement mantle fatigue failure in total hip replacement: Experimental and computational testing

Jonathan R.T. Jeffers[a], Martin Browne[a], Alexander B. Lennon[b],
Patrick J. Prendergast[b], Mark Taylor[a],*

[a]*Bioengineering Sciences Research Group, University of Southampton, Southampton, SO17 1BJ, United Kingdom*
[b]*Trinity Centre for Bioengineering, Trinity College, Dublin 2, Ireland*

Abstract

One possible loosening mechanism of the femoral component in total hip replacement is fatigue cracking of the cement mantle. A computational method capable of simulating this process may therefore be a useful tool in the preclinical evaluation of prospective implants. In this study, we investigated the ability of a computational method to predict fatigue cracking in experimental models of the implanted femur construct. Experimental specimens were fabricated such that cement mantle visualisation was possible throughout the test. Two different implant surface finishes were considered: grit blasted and polished. Loading was applied to represent level gait for two million cycles. Computational (finite element) models were generated to the same geometry as the experimental specimens, with residual stress and porosity simulated in the cement mantle. Cement fatigue and creep were modelled over a simulated two million cycles. For the polished stem surface finish, the predicted fracture locations in the finite element models closely matched those on the experimental specimens, and the recorded stem displacements were also comparable. For the grit blasted stem surface finish, no cement mantle fractures were predicted by the computational method, which was again in agreement with the experimental results. It was concluded that the computational method was capable of predicting cement mantle fracture and subsequent stem displacement for the structure considered.
© 2006 Elsevier Ltd. All rights reserved.

Keywords: Bone cement; Fatigue; Finite element; Continuum damage mechanics; Hip replacement

1. Introduction

Follow-up studies of the Charnley total hip replacement report 'remarkable durability' of the reconstruction, with most functioning for over thirty years (Callaghan et al., 2004; Wroblewski et al., 2001). The success of the Charnley prosthesis has not prevented new designs being released on the market—the National Joint Registry for England and Wales reports 47 different cemented prosthesis designs currently in use.[1] New designs are not always successful, for example the Capital prosthesis, released in 1991 by 3 M, had poor short-term survival rates that led to a hazard warning being issued seven years later (UK Medical Devices Agency Hazard Notice HN9801) and its removal from the market (Massoud et al., 1997). Therefore, despite the success of the Charnley total hip replacement, preclinical testing against known failure scenarios may still be necessary to prevent potentially dangerous designs reaching clinical trials.

Failure of the reconstructed hip is usually caused by component loosening (Havelin et al., 2000; Herberts et al., 2002; Lucht, 2000; Puolakka et al., 2001), which can be caused by several mechanisms. One of these is fatigue fracture of the cement mantle, identified by Jasty et al. (1990) in their retrieval study of 16 femora. Further evidence of this loosening mechanism comes from radiographic analysis (Stauffer, 1982), inspection of ex vivo cement mantle pieces (Topoleski et al., 1990) and in vitro studies (McCormack et al., 1999). Factors that may

*Corresponding author. Tel.: +44 2380 597660; fax: +44 2380 593016.
E-mail address: m.taylor@soton.ac.uk (M. Taylor).
[1]National Joint Registry 1st Annual Report (Sept 2004), available from www.njrcentre.org.uk

influence the fatigue processes within bone cement include porosity, residual stress and viscoelastic effects. Pores in the cement have been cited as being influential in the fatigue process, by initiating microcracks and facilitating their coalescence (Jasty et al., 1990; McCormack et al., 1999; Topoleski et al., 1990). Residual stress, generated during the polymerisation of the cement, may also be influential as stresses in the order of 10 MPa have been documented, capable of generating damage in the cement prior to loading (Roques et al., 2004). Cement creep has been suggested as a possible mechanism whereby stresses in the cement are relaxed, and this may in turn have some bearing on the fatigue process (Verdonschot and Huiskes, 1997a).

Given that cement mantle fatigue is a possible loosening mechanism, preclinical evaluation of this phenomenon is useful and one method of performing this is via computational (finite element) simulation. By simulating cement mantle fatigue in finite element models, a number of studies have investigated various aspects of total hip replacement. Using physiological implanted femur finite element models, Verdonschot and Huiskes (1997b) investigated the effect of unbonding the stem/cement interface and Stolk et al. (2002) used a similar method to determine the effect stair climbing had on fatigue within the cement. Confidence in computational methods, such as these, will be strengthened if results obtained from them are about the same as those from experimental testing. In this respect, Stolk et al. (2004) simulated fatigue and creep of bone cement under uniaxial tensile fatigue loads, and predicted similar fatigue lives and creep strains to experimental data. Using a similar method, Jeffers et al. (2005a) included cement porosity and were able to reproduce experimental S–N curves for uniaxial tensile and 4-point bend fatigue. When applied to physiological models, however, experimental comparisons have not been as successful as for the simple structures. Stolk et al. (2003) applied the computational method to implanted femur models of two different prosthesis designs, and were able to generate similar levels of prosthesis migration and damage in the cement. However, the computational analysis required 20×10^6 simulated load cycles to generate the results observed experimentally after 2×10^6 load cycles. This discrepancy was attributed to the absence of pores and residual stress induced pre-cracks in the cement mantle of the finite element models.

The aim of the current study is to simulate fatigue in finite element models of a simplified implanted femur structure, and provide good comparisons, in terms of damage locations and stem displacements, with experimental specimens subject to a similar number of load cycles. To realise this, the computational simulation of fatigue includes the influence of cement creep, residual stress and porosity. Different stem surface finishes are included to further test the computational method. A simplified implanted femur geometry is used so that any cement cracking will be visible during the testing process.

Successful comparisons for this structure should allow for increased confidence in continuum damage mechanics/finite element based preclinical testing.

2. Materials and methods

2.1. Experimental specimens

Each experimental specimen consisted of a steel stem fixed in an aluminium femur with acrylic bone cement (Fig. 1a). The aluminium femur consisted of a back and front cover, which fitted together to enclose the stem and cement. This was based on a similar model developed by Lennon et al. (2003), and had a similar second moment of area measured at the mid section of the stem ($25,000 \, \text{mm}^4$). Cancellous bone was modelled with 3 mm thick solid rigid polyurethane foam strips (Sawbones Europe AB, Sweden), fixed to the aluminium with cyanoacrylate adhesive. Windows in the side of the aluminium femur model allowed visualisation of the cement during fatigue loading. The stem geometry was taken from measurements of a Charnley prosthesis, and had a polished surface finish (mean Ra = 0.1 μm). Clamping the stem in position left a uniform 5 mm cavity for the bone cement. The bone cement (CMW-1, DePuy CMW, UK) was vacuum mixed as per manufacturers instructions, and injected into the cement cavity from the distal end using a cement gun. This was performed with the top aluminium cover removed, and a polyethylene (PE) sheet with steel backing plate covering the cement cavity. Specimens were left to cure overnight. Once cured, the PE sheet was removed and the stem removed and replaced in the cement mantle to ensure a fully unbonded stem/cement interface. The front aluminium cover was put on the specimens before testing. Three such specimens were built.

One further specimen was fabricated, to simulate a bonded stem/cement interface. This was achieved as described above, but with a grit blasted femoral stem (mean Ra 2.2 μm) and without removing the stem from the cement.

2.2. Mechanical testing

A load horse was designed to allow a joint reaction force of 2.5 kN to be applied at 10° to the vertical, and an abductor force of 1.5 kN at an angle of 15° to the vertical (Fig. 1b). This corresponded to 3.5 times bodyweight loading (assuming bodyweight equal to 700 N), and was similar to the loading used by Lennon et al. (2003). A sinusoidal compressive load was applied to the head of the horse for 2 million cycles, at an R-ratio of 0.1 and a frequency of 5 Hz. Testing was performed in air at room temperature. Actuator displacement was recorded throughout the test. After testing, specimens were analysed by computed tomography (CT) and dye penetrant to check the levels of porosity and microcracking, respectively.

2.3. Computational analysis

Four finite element models of the experimental specimens were generated (Fig. 1c). Each consisted of 27,500 4-node tetrahedral elements, 9200 of which were in the cement mantle. The volume of the cement mantle was $5800 \, \text{mm}^3$, giving an average element volume of $0.6 \, \text{mm}^3$, which satisfied a previous mesh sensitivity study (Jeffers et al., 2005a). The material properties used in the finite element models are given in Table 1. A spatial distribution of pores in the cement mantle was generated for each finite element model using experimental data and a Monte Carlo simulation (Volume of *elements containing* pores was 3.3%, 6.4%, 10.6% and 16.5% for the four finite element models. Note that volume of pores would be smaller than these values as pores were simulated within the element). Elements simulating pores were assigned randomly, and the theoretical elastic solution for a spherical cavity was used to simulate the stress concentration (2.05σ), as has been described in a number of previous studies (Harrigan and Harris, 1991; Harrigan et al., 1992; Jeffers
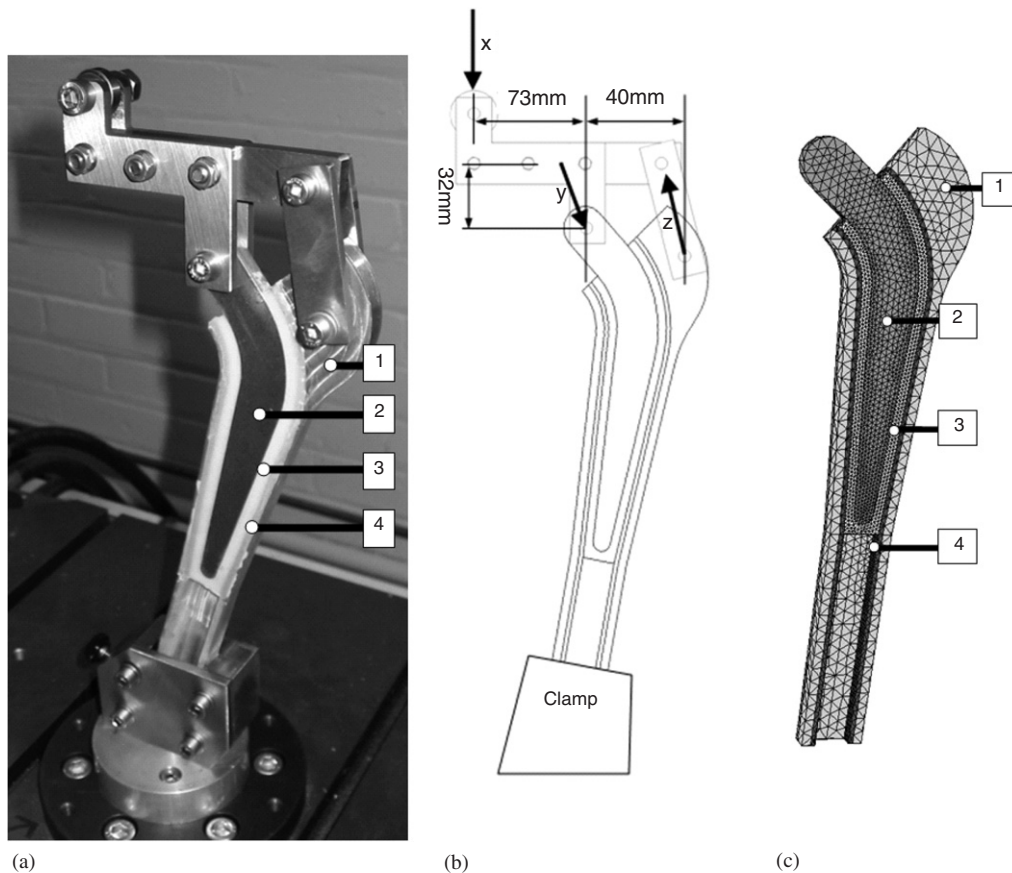
Fig. 1. (a) Schematic of experimental specimen showing (x) applied load, (y) hip contact force at 10° to vertical and (z) abductor force at 15° to the vertical. (b) Experimental model fixed in testing machine with the front cover removed and (c) the finite element model. The following are identified: (1) aluminium cortex, (2) stem, (3) bone cement and (4) polyurethane foam.

Table 1
Material properties used in the finite element models

Material	Young's modulus (GPa)	Poisson's ratio
Steel	240.0	0.3
Aluminium	73.0	0.3
Polyurethane foam	2.0	0.28
Cement	2.4	0.3

et al., 2005a; Lennon et al., 2003). To simulate residual stress in the cement, an adapted version of the method presented by Baliga et al. (1992) was used to calculate heat generation as a function of temperature and fraction of monomer polymerised. Once polymerisation was complete, shrinkage stresses were determined assuming shrinkage from the maximum temperature attained by each element. (see Lennon and Prendergast (2002) for full details). The residual stress field had a peak value of 8 MPa distal to the prosthesis tip.

Cement fatigue and creep were simulated using the continuum damage mechanics approach originally developed by Verdonschot and Huiskes (1997b), and briefly summarised here. Every element in the cement was assigned a damage variable, d. At the beginning of the analysis, d was set to zero for all elements. While damage may occur continuously or otherwise in cement subject to fatigue loading, it is not necessary to simulate every loading cycle. An iterative solution procedure was employed, each iteration representing the action of tens to tens of thousands of loading cycles depending on the stress level in the elements.

At the beginning of each iteration, the load was applied to the finite element model and the maximum tensile stress calculated for each element by the finite element solver. Based on this stress level, the number of cycles to failure (N_f) was calculated for every element in the cement mantle from a uniaxial S–N curve. The number of cycles simulated in the iteration was then determined, based on a predefined percentage (20%, found to be acceptable with a convergence study) of the lowest N_f of the elements in the mesh. Damage was incremented for each element according to the linear Palmgren-Miner rule: $\Delta d = \Delta n/N_f$, where n was the number of cycles simulated to date, and added to the damage already accumulated (d) for each element. When $d \geqslant 0.9$, the element was deactivated (modulus reduced to zero) and the load transferred to the surrounding elements. Elements containing a pore were subjected to a stress concentration (2.05σ, described above) and N_f calculated based on the elevated stress. At the end of each iteration, cement creep strain was calculated for every element in the cement using an empirical creep law (Jeffers et al., 2005b), maximum tensile stress level, the number of cycles simulated in the iteration and the number of loading cycles completed at the beginning of the iteration. Creep strains and any elements to be deactivated were then returned to the solver which applied the load again for the next iteration. It took about 120 such iterations to simulate two million cycles; each iteration took approximately two hours. For full details of the computational method, please see Jeffers et al. (2005a).

Four finite element models, each with a unique pore distribution were generated as described above. Three models had an unbonded stem/cement interface (frictional coefficient = 0.25) to represent the experimental specimens with a polished stem finish; the fourth had a bonded stem/cement interface to represent the grit blasted stem finish.

3. Results

3.1. Unbonded stem/cement interface conditions

Complete cement mantle fractures occurred in all three unbonded experimental specimens (polished stem finish) at the distal end of the stem (Fig. 2a–c). From the actuator displacement data and visual inspection, the number of load cycles to fracture could be determined (Table 2). The earliest distal fracture occurred at 300 load cycles, or 60 s into the test, and the latest fractures had occurred by 100,000 cycles or 5.5 h. In two cases the cement fractured at both the medial and lateral sides (Figs. 2a and c), but, in one case, it fractured at the lateral side only (Fig. 2b). Further inspection revealed that, in this case, the cyanoacrylate adhesive bonding the cancellous bone substitute to the aluminium had failed, leading to migration of the medial cement rather than fracture at the distal end. This debonding was not evident in the other specimens. Micrographs of the fracture surfaces revealed evidence of fatigue failure originating at the stem/cement interface (Fig. 3a). Although complete fractures only occurred at the distal tip of the stem, micro damage was observed throughout the cement in all the specimens (Fig. 3b and c), mainly originating from the interfaces and pores within the cement. CT scanning revealed the levels of porosity in the cement varied from about 0.8% (Fig. 4a) to about 15% (Fig. 4b) by volume, similar to the levels simulated in the finite element models (which were 3.3–16.5%).

Complete cement mantle fractures also occurred in the finite element models, in a similar location to the experimental specimens (Fig. 5a–c). These distal cracks originated at the stem/cement interface and propagated outwards. Plotting damage as a function of loading cycles revealed a clear step in the damage accumulation

corresponding to these distal cement fractures, which occurred between 1000 and 10,000 load cycles (Fig. 6). Finite element model (a), with the lowest pore fraction (3.3% by volume) had a complete cement mantle fracture in the proximo-medial cement (circled in Fig. 5a). This proximal fracture manifested itself as a sharp increase in damage accumulation rate, highlighted in Fig. 6.

The fractures in the distal cement displayed characteristic angles of 70–75° to the axis of the stem (Fig. 2). It was therefore not surprising that the maximum principal stress vectors in the finite element models when the load was applied were at 90° to this angle. However, the maximum principal stress vectors in the residual stress field were in the plane of the final fracture, suggesting that, for the structure considered, the residual stresses were not responsible for the fractures in the experimental specimens. The distal stresses, not including the effects of a pore were high—in the region of 30 MPa, indicating that the applied load was the dominant cause of failure. Residual stresses in the cement may not have been critical in the distal cement, but were likely to have contributed to the proximal fracture circled in Fig. 5a. In this section of cement, the residual stresses were at 90° to the plane of the fracture, with magnitude of 4–5 MPa.

Inducible displacement at the head of the stem (i.e. displacement recovered when implant was unloaded) was

Table 2
Number of cycles to distal fracture of cement for the four experimental specimens

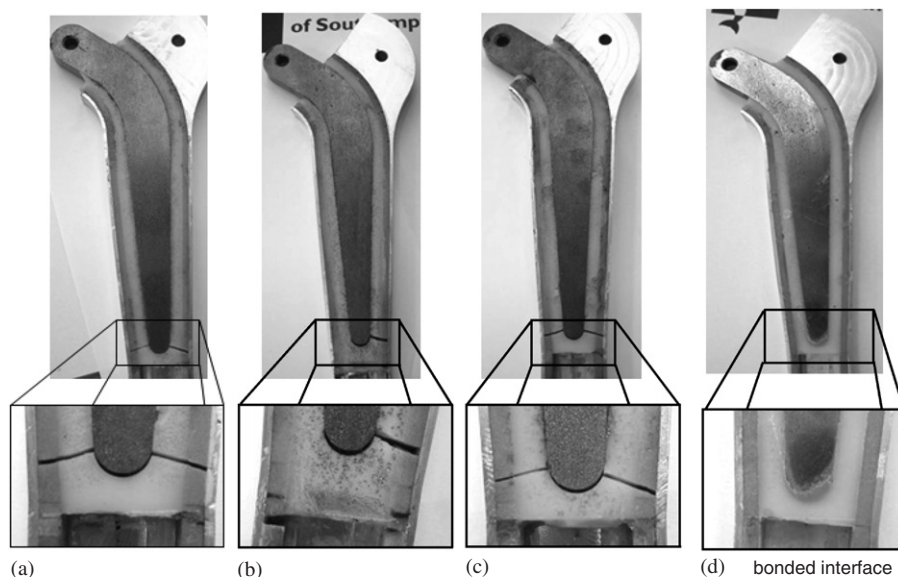| Specimen	Load cycles to distal fracture
A (polished stem)	300
B (polished stem)	100,000
C (polished stem)	15,000
D (grit-blasted stem)	No fracture

Fig. 2. Cement mantle fractures in the four different specimens after 2 million load cycles for the polished stem finish (a–c) and grit blasted stem finish (d).
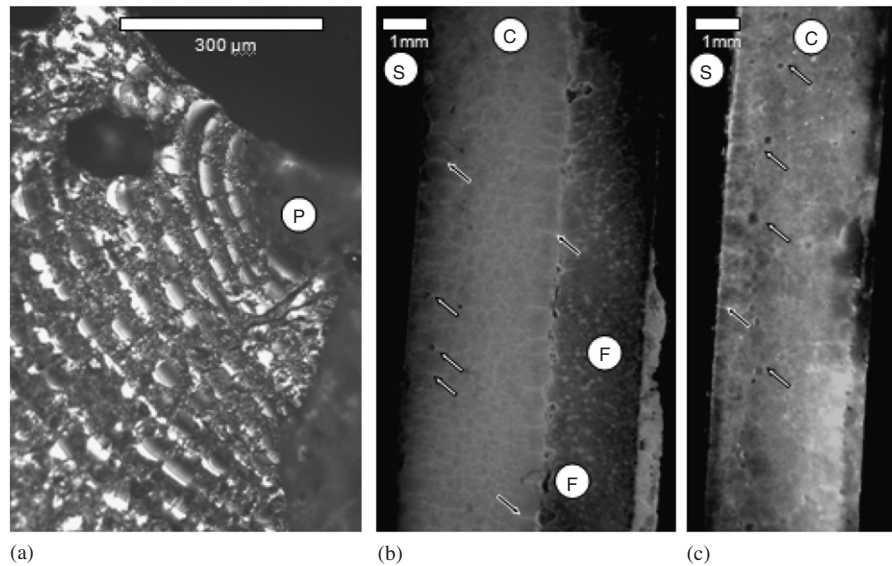
Fig. 3. (a) Optical micrograph of fatigue striations originating from pore (P) at the stem/cement interface: unbonded stem/cement interface. (b) Dye penetrant staining of the proximolateral cement of an unbonded specimen and (c) the distolateral cement of the bonded specimen identifying some of the microcracking occurring at the interface (black arrows) and from pores (white arrows). S-stem, C-cement, F-polyurethane foam.
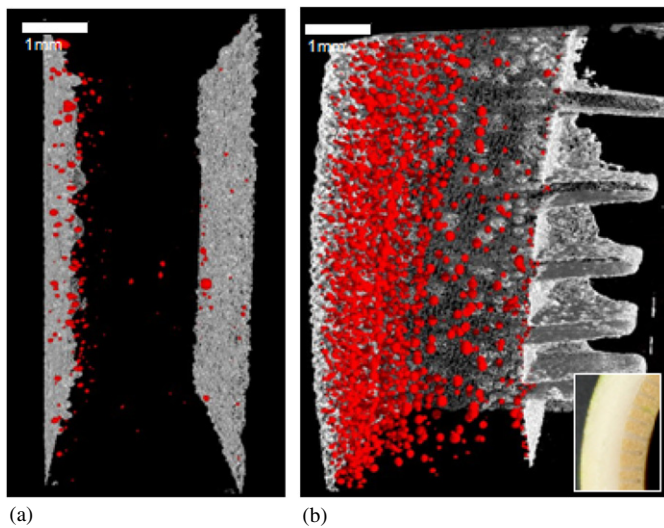

Fig. 4. CT scans of the cement of two different specimens: (a) distolateral cement with low porosity (0.8% by volume); and (b) proximomedial cement with high porosity (15% by volume). The fins in (b) correspond to the cuttings made in the polyurethane foam strips to fit the curve of the specimen (see inset). Note higher density of pores towards the stem/cement interface in both cases.

recorded for both the experimental specimens and the finite element models, and there was reasonably good agreement between both sets of data (Fig. 7). After the initial 500,000 load cycles, inducible displacement remained relatively constant, apart from the 3.3% pore fraction finite element model that experienced a drop in inducible displacement from 1 mm to 0.8 mm at about 1 million load cycles. This drop in displacement was caused by the proximo-medial cement mantle fracture, circled in Fig. 5a.

3.2. Bonded stem/cement interface conditions

No fractures were observed anywhere in the cement mantle of the experimental specimen with the grit blasted stem finish (bonded interface), as shown in Fig. 2d. However, microcracking, especially along the lateral side was evident with the dye penetrant analysis (Fig. 3c), originating from pores and defects at the interfaces. Similar results were generated for the finite element model of the bonded stem/cement interface (Fig. 5d), no distal fractures were predicted, but damage was generated elsewhere in the cement as can be seen in Fig. 5d. This is more clearly illustrated in Fig. 6, where the damage can be seen to begin to rise at about 1e6 load cycles. Inducible displacements were comparable between computational model and experimental specimen throughout the loading history, and of slightly lower magnitude to the unbonded stem/cement interface data (shown in Fig. 7).

4. Discussion

The current study has demonstrated that fatigue can be simulated in finite element models of a simplified implanted femur structure. Fracture locations and stem displacement were similar, even for different stem/cement interface conditions. Cement fractures were predicted in a similar timescale to those observed experimentally, but this would have also been the case were porosity and residual stress omitted, as the high distal stresses were dominated by the applied load. However, were porosity and residual stress not included, no damage would have been simulated in other areas in the cement. For the bonded analysis, no damage would have been simulated at all. The dye penetrant revealed damage at locations other than the
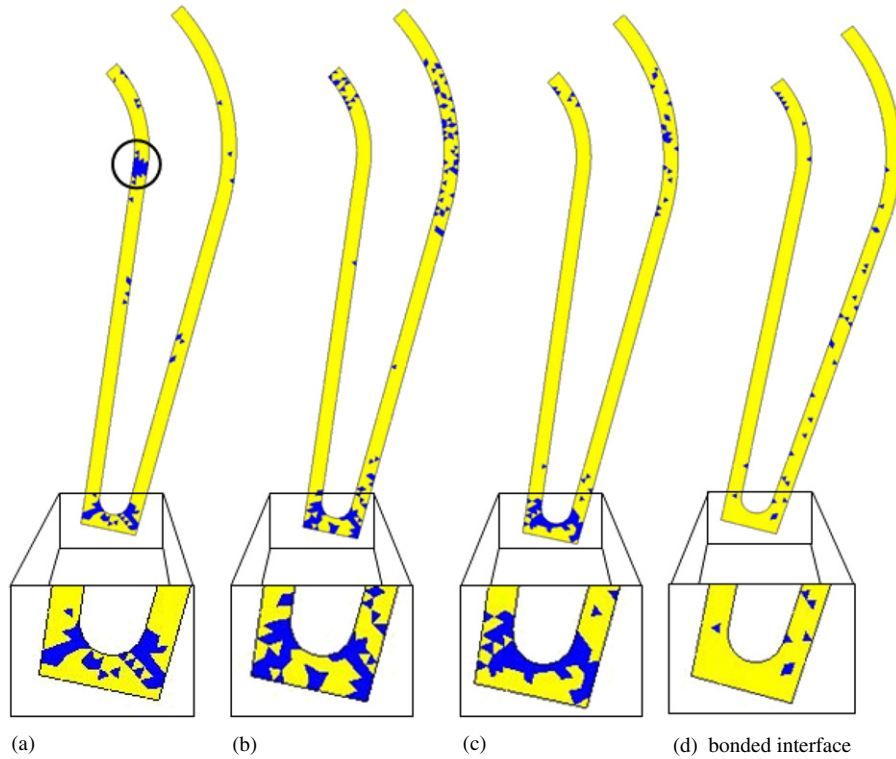
Fig. 5. Damage in the cement mantle after 2 million load cycles as predicted by the computational method for: (a) 3.3% pore fraction with unbonded interface; (b) 16.5% pore fraction with unbonded interface; (c) 6.4% pore fraction with unbonded interface; and (d) 10.6% pore fraction with bonded interface. Proximo-medial fracture is circled in (a).
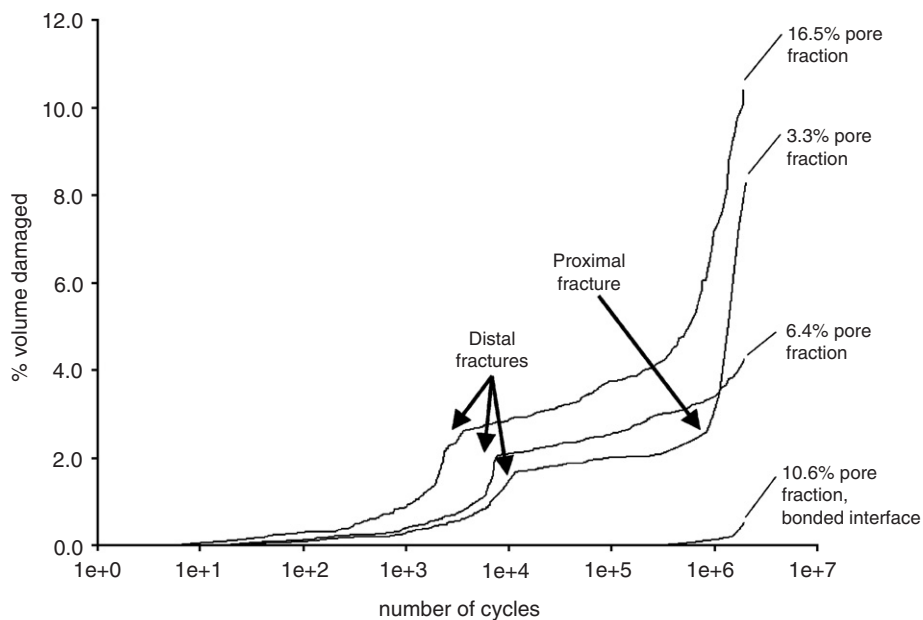

Fig. 6. Damage in the cement as a function of loading cycles for the four finite element models.

distal tip for all specimens, which was also found by Lennon et al. (2003) for similar models. The variability in number of cycles to distal fracture is another feature that would be lost by omitting porosity. These points suggest that including residual stress and porosity may generate

improved results when applied to the physiological reconstruction.

There were, however, a number of limitations with the computational method. Elements were deactivated to simulate cement damage, and the elements therefore lost
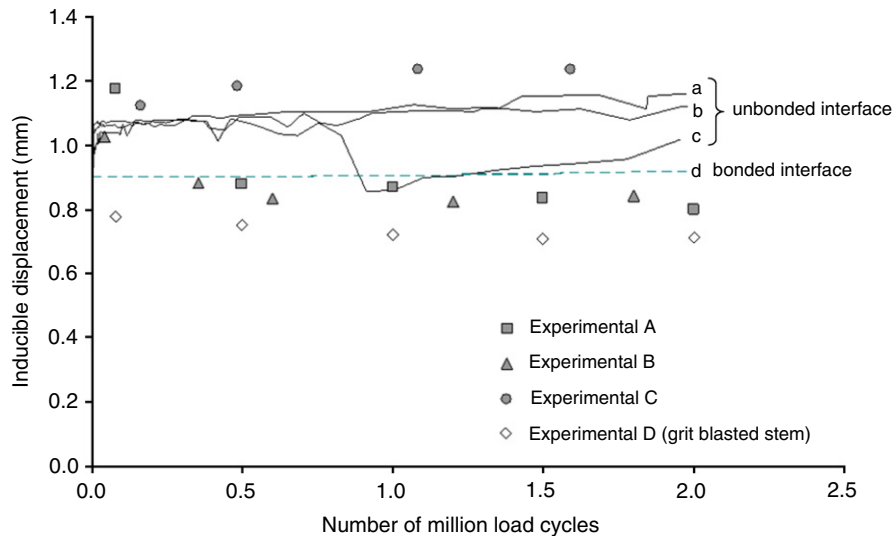
Fig. 7. Experimental and computational inducible displacement as a function of time. Solid/dashed lines represent the computational results: (a) 16.5% pore fraction; (b) 6.4% pore fraction; (c) 3.3% pore fraction; and (d) 10.6% pore fraction with bonded interface.

their capacity to transfer load in all orientations, and not just in the plane normal to the simulated crack. While this approach may be acceptable for constant amplitude loading conditions, it may not be possible to simulate the spectrum of loading experienced in vivo (i.e. gait, stair ascent, stair decent, sitting, standing, etc.). Stolk et al. (2003) addressed this limitation by employing a multiaxial damage algorithm capable of reducing the element modulus in the plane normal to the simulated crack only. This has been further enhanced by Lennon and Prendergast (2004) to enable load transfer upon crack closure.

The computational method calculated fatigue based on a uniaxial tensile fatigue curve. The experimental specimens used in the current study dictated that cement stresses would be essentially uniaxial in nature, and the limitations in using this method for cement under triaxial stress may not have been highlighted. This may be an issue as the in vivo cement stress field is triaxial in nature, and cement under triaxial loading can experience notably different fatigue characteristics to that under uniaxial loading (Murphy and Prendergast, 2003). For future applications, a possible means to overcome this limitation would be to use an equivalent stress value in the calculation of cement fatigue, for example the von Mises or Sines stress formulations. The linear damage accumulation law employed was also a limitation, as this did not take into account the order of different applied loads. For metal alloys under completely reversed loading, the linear law has been unsatisfactory when modelling a low-to-high sequence or a high-to-low sequence (Fatemi and Yang, 1998). This may also be the case for bone cement, as the non-linearity of damage accumulation has been documented (Murphy and Prendergast, 2001). Another limitation was that the S–N curve used to calculate damage was generated under simulated in vivo conditions (aged in Saline and tested at 37 °C, see Jeffers et al., 2005b), while the experimental tests were performed in air at room temperature. In his review article, Lewis (2003) summarised that the fatigue life of cement tested under simulated in vivo conditions was superior to that tested in air. This limitation would not apply were the computational method applied to the in vivo situation. Using the Monte Carlo simulation to generate a random distribution of pores in the cement was also a limitation, as the CT scanning revealed that pore density was greater towards the stem/cement interface. This could be resolved by introducing a bias factor into the pore distribution algorithm to increase the likelihood of pores closer to the stem.

A number of studies have suggested that pre-load damage exists in the cement mantle as a result of the shrinkage during cement polymerisation, and that this may influence the overall fatigue behaviour (Britton et al., 2003; Mann et al., 2004; Orr et al., 2003). It is therefore probable that damage was present in the experimental specimens prior to loading. Although this was not modelled explicitly, the residual stress field and porosity combined to generate damage in the first load cycle. The residual stress field had a mean value of 4 MPa and a peak value of 8 MPa, while the stress concentrating effect of a pore effectively doubled the stress in elements. In numerous cases, these effects, along with the applied load, were sufficient to cause damage in the first load cycle that would not have occurred due to the applied load alone. With regard to the dye penetrant analysis, some of the microdamage may have been present in the cement prior to loading, but a study of similar experimental specimens by Lennon et al. (2003) revealed that significant microdamage was also generated throughout the cement as a result of the applied fatigue load. This is consistent with the results of the current study.

One of the most interesting outcomes of the current study, and one that deserved further investigation, was the proximo-medial cement mantle fracture in one of the finite

element models (circled in Fig. 5a). A stress analysis of an almost identical structure by Lennon et al. (2003) revealed a slight stress concentration in this region, but not enough to cause failure within two million cycles. At first it seemed unlikely that porosity was the cause, as the Monte Carlo simulation generated the least number of pores for this particular model (3.3% pore fraction). However, upon closer inspection, we found the random distribution of pores had created a localised high pore density in this region. The subsequent fracture highlighted two features of the study—firstly that the pore distribution was equally important as the number of pores in the cement. This was also commented on by Murphy and Prendergast (2000) in a uniaxial tensile fatigue study of hand-mixed versus vacuum-mixed specimens. Secondly, that a degree of variability was generated by introducing unique pore distributions to different finite element models. This was also demonstrated by Jeffers et al. (2005a) and Lennon and Prendergast (2004) for bone cement under 4-point bend and tensile fatigue loads.

As the experimental specimen design was based on that of Lennon et al. (2003), there should be similarities in the results. Inducible displacement of the stem was of a similar magnitude, between 0.8 and 1.2 mm after 2 million cycles (Fig. 7). Areas of the cement susceptible to damage were also similar. For an unbonded stem/cement interface, Lennon et al. (2003) predicted elevated stresses in the regions where damage occurred in the current study (Fig. 5). Lennon et al. (2003) also monitored the micro-crack accumulation in the cement by surface staining with dye, and found an increased tendency for damage accumulation with an unbonded stem/cement interface. This is consistent with our finite element results, where more damage was predicted in the unbonded models, even neglecting the distal fractures. In the computational part of the present study, the coefficient of friction was selected as 0.25, the same as that used by Lennon et al. (2003). Given that there was increased tendency for damage in the unbonded models, it is likely that a lower coefficient of friction would increase the damage accumulation rates predicted in the finite element models, with the worst case scenario being a frictionless analysis.

The results generated by the computational method were very encouraging, but did not predict the lateral only fracture observed in Fig. 2b. As mentioned in Section 3.1, shear failure of the cyanoacrylate adhesive on the medial side led to subsidence of the medial cement mantle and polyurethane foam rather than cement fracture (see Fig. 2b). No provision was made for this in the finite element analysis—all interfaces, except the stem/cement interface, were modelled as completely bonded. This was not necessarily a limitation with the method, but it does emphasise the importance of how the results are interpreted. For example, in the same way no provision was made for failure of the cyanoacrylate adhesive, no provision was made for abrasion at the stem/cement interface. Verdonschot and Huiskes (1998) have shown

that a debonded grit blasted stem surface finish can abrade the cement at the stem/cement interface, producing more acrylic cement debris than a debonded polished stem, and potentially have an adverse effect on the survival of the reconstruction. Thus the present study does not advocate a grit blasted stem surface finish over a polished finish; the computational method may be used to test against cement mantle fatigue only, and in preclinical testing the results must be interpreted alongside those for other loosening mechanisms.

The continuum damage mechanics approach is a considerable simplification of the fatigue processes that occur in bone cement, but is arguably the only current practical means to assess the entire cement mantle using numerical methods. The results generated by this method have been good—experimental data has been reproduced for tensile (Lennon and Prendergast, 2004; Stolk et al., 2004) and 4-point bend specimens (Jeffers et al., 2005a). When applied to the physiological reconstruction, the damage patterns and stem migration were well modelled (Stolk et al., 2003). The results of the present study suggests that the continuum method is also capable of predicting fatigue locations in a comparable timescale to experimental data, and by incorporating Monte Carlo methods can generate a range of results rather than a single deterministic one. The present results, along with those from these prior studies, should strengthen the use of finite element/ continuum damage mechanics in preclinical testing.

Acknowledgements

References

Baliga, B.R., Rose, P.L., Ahmed, A.M., 1992. Thermal modelling of polymerizing polymethylmethacrylate, considering temperature-dependant heat generation. Journal of Biomechanical Engineering 114, 251–259.

Britton, J.R., Walsh, L.A., Prendergast, P.J., 2003. Mechanical simulation of muscle loading on the proximal femur: analysis of cemented femoral component migration with and without muscle loading. Clinical Biomechanics 18, 637–646.

Callaghan, J.J., Templeton, J.E., Liu, S.S., Pedersen, D.R., Goetz, D.D., Sullivan, P.M., Johnson, R.C., 2004. Results of Charnley total hip arthroplasty at a minimum of thirty years. Journal of Bone and Joint Surgery—American Volume 86-A (4), 690–695.

Harrigan, T.P., Harris, W.H., 1991. A three dimensional non linear finite element study of the effect of cement–prosthesis debonding in cemented femoral total hip components. Journal of Biomechanics 24 (11), 1047–1058.

Harrigan, T.P., Kareh, J.A., O'Connor, D.O., Burke, D.W., Harris, W.H., 1992. A finite-element study of the initiation of failure of fixation in cemented femoral total hip components. Journal of Orthopaedic Research 10 (1), 134–144.

Havelin, L.I., Engesaeter, L.B., Espehaug, B., Furnes, O., Lie, S.A., Vollset, S.E., 2000. The Norwegian arthroplasty register—11 years and 73,000 arthroplasties. Acta Orthopaedica Scandinavica 71 (4), 337–353.

Herberts, P., Malchau, H., Garellick, G., Soderman, P., Eisler, T., 2002. Prognosis of total hip replacement, Goteborg University. Available from ⟨http://www.jru.orthop.gu.se⟩.

Fatemi, A., Yang, L., 1998. Cumulative fatigue damage and life prediction theories: a survey of the state of the art for homogeneous materials. International Journal of Fatigue 20 (1), 9–34.

Jasty, M., Davies, J.P., O'Connor, D.O., Burke, D.W., Harrigan, T.P., Harris, W.H., 1990. Porosity of various preparations of acrylic bone cements. Clinical Orthopaedics and Related Research 259, 122–129.

Jeffers, J.R.T., Browne, M., Roques, A., Taylor, M., 2005a. On the importance of considering porosity when simulating the fatigue of bone cement. Journal of Biomechanical Engineering 127 (4), 563–570.

Jeffers, J.R.T., Browne, M., Taylor, M., 2005b. Damage accumulation, fatigue and creep of vacuum mixed bone cement. Biomaterials 26 (27), 5532–5541.

Lennon, A.B., Prendergast, P.J., 2002. Residual stress due to curing can initiate damage in porous bone cement: experimental and theoretical evidence. Journal of Biomechanics 35 (3), 311–321.

Lennon, A.B., Prendergast, P.J., 2004. Modelling damage growth and failure in elastic materials with random defect distributions. Mathematical Proceedings of the Royal Irish Academy 104A (2), 155–171.

Lennon, A.B., McCormack, B.A.O., Prendergast, P.J., 2003. The relationship between cement fatigue damage and implant surface finish in proximal femoral prostheses. Medical Engineering and Physics 25, 833–841.

Lewis, G., 2003. Fatigue testing and performance of acrylic bone–cement materials: state-of-the-art review. Journal of Biomedical Materials Research Part B-Applied Biomaterials 66B (1), 457–486.

Lucht, U., 2000. The Danish hip arthroplasty register. Acta Orthopaedica Scandinavica 71 (5), 433–439.

Mann, K.A., Gupta, S., Race, A., Miller, M.A., Cleary, R.J., Ayers, D.C., 2004. Cement microcracks in thin-mantle regions after in vitro fatigue loading. Journal of Arthroplasty 19 (5), 605–612.

Massoud, S.N., Hunter, J.B., Holdsworth, B.J., Wallace, W.A., Juliusson, R., 1997. Early femoral loosening in one design of cemented hip replacement. Journal of Bone and Joint Surgery—British Volume 79B (4), 603–608.

McCormack, B.A.O., Prendergast, P.J., O'Dwyer, B., 1999. Fatigue of cemented hip replacements under torsional loads. Fatigue and Fracture of Engineering Materials and Structures 22 (1), 33–40.

Murphy, B.P., Prendergast, P.J., 2000. On the magnitude and variability of the fatigue strength of acrylic bone cement. International Journal of Fatigue 22, 855–864.

Murphy, B.P., Prendergast, P.J., 2001. The relationship between stress, porosity and nonlinear damage accumulation in acrylic bone cement. Journal of Biomedical Materials Research 59, 646–654.

Murphy, B.P., Prendergast, P.J., 2003. Multi-axial fatigue failure of orthopaedic bone cement—experiments with tubular specimens. Journal of Materials Science—Materials in Medicine 14 (10), 857–861.

Orr, J.F., Dunne, N.J., Quinn, J.C., 2003. Shrinkage stresses in bone cement. Biomaterials 24 (17), 2933–2940.

Puolakka, T.J.S., Pajamaki, K.J.J., Halonen, P.J., Pulkkinen, P.O., Paavolainen, P., Nevalainen, J.K., 2001. The Finnish arthroplasty register—report of the hip register. Acta Orthopaedica Scandinavica 72 (5), 433–441.

Roques, A., Browne, M., Taylor, A., New, A., Baker, D., 2004. Quantitative measurement of the stresses induced during polymerisation of bone cement. Biomaterials 25 (18), 4415–4424.

Stauffer, R.N., 1982. Ten-year follow up study of total hip replacement. Journal of Bone and Joint Surgery—American Volume 64-A (7), 983–990.

Stolk, J., Verdonschot, N., Huiskes, R., 2002. Stair climbing is more detrimental to the cement in hip replacement than walking. Clinical Orthopaedics and Related Research 405, 294–305.

Stolk, J., Maher, S.A., Verdonschot, N., Prendergast, P.J., Huiskes, R., 2003. Can finite element models detect clinically inferior cemented hip implants? Clinical Orthopaedics and Related Research 409, 138–150.

Stolk, J., Verdonschot, N., Murphy, B.P., Prendergast, P.J., Huiskes, R., 2004. Finite element simulation of anisotropic damage accumulation and creep in acrylic bone cement. Engineering Fracture Mechanics 71 (4–6), 513–528.

Topoleski, L.D.T., Ducheyne, P., Cuckler, J.M., 1990. A fractographic analysis of in vivo poly(methyl methacrylate) bone–cement failure mechanisms. Journal of Biomedical Materials Research 24 (2), 135–154.

Verdonschot, N., Huiskes, R., 1997a. Acrylic cement creeps but does not allow much subsidence of femoral stems. Journal of Bone and Joint Surgery—British Volume 79-B (4), 665–669.

Verdonschot, N., Huiskes, R., 1997b. The effects of cement-stem debonding in THA on the long-term failure probability of cement. Journal of Biomechanics 30 (8), 795–802.

Verdonschot, N., Huiskes, R., 1998. Surface roughness of debonded straight-tapered stems in cemented THA reduces subsidence but not cement damage. Biomaterials 19 (19), 1773–1779.

Wroblewski, B.M., Siney, P.D., Fleming, P.A., 2001. Charnley low-frictional torque arthroplasty in patients under the age of 51 years—follow up to 33 years. Journal of Bone and Joint Surgery—British Volume 84-B (4), 540–543.